# TECHNICAL MEMORANDUM

## X-248

AN ANALYSIS OF THE STABILITY OF SPINNING DISKS

DURING ATMOSPHERE REENTRY

By John D. Bird and Charles P. Llewellyn

Langley Research Center
Langley Field, Va.

Declassified March 15, 1962

NATIONAL AERONAUTICS AND SPACE ADMINISTRATION

WASHINGTON                                    March 1960

NATIONAL AERONAUTICS AND SPACE ADMINISTRATION

TECHNICAL MEMORANDUM X-248

AN ANALYSIS OF THE STABILITY OF SPINNING DISKS

DURING ATMOSPHERIC REENTRY*

By John D. Bird and Charles P. Llewellyn

SUMMARY

An analysis of the dynamic stability of spinning disks during atmospheric reentry was made by numerical integration of five-degree-of-freedom nonlinear equations of motion on an IBM type 704 electronic data processing machine and by study of linearized equations of motion. It was established that high rates of deceleration may be obtained on reentry as a result of the instability which occurs at high dynamic pressures for sufficiently low spin rates. Considerable dispersion in impact point may occur because of the relatively high lift capability of disk forms.

INTRODUCTION

For a period of years, spin about the longitudinal axis has been employed to stabilize various forms of bullets and shells with a marked degree of success. However, little attention has been given to the dynamic behavior of flattened disk forms that travel edgewise and are stabilized by spin about an axis normal to the direction of flight. The purpose of this investigation was to study the use of such spinning disk bodies for reentry applications. In this work it was intended to explore the behavior of spinning disk forms, determine the significance of spin effects, and to study the dynamic-stability properties of such configurations. In order to do this a series of calculations of the reentry of such bodies were made by use of an IBM type 704 electronic data processing machine for various conditions and configurations. Newtonian aerodynamics were employed. Additional work was done by linear analysis in which roots of the stability equations were determined for a range of conditions.

SYMBOLS

The results are referred to the axes shown in figure 1 in which positive directions of moments and velocities are determined by the

_____
*
Title, Unclassified.

2

right-hand rule.   The symbols and coefficients are defined as follows:

| | |
|---|---|
| $X, Y, Z$ | reference axes with origin located at the body center of mass (these axes are not body axes in that they permit the body to spin about the X-axis with respect to the Y- and Z-axes) |
| $x, y, z$ | space reference frame with origin fixed at surface of Earth |
| $u, v, w$ | velocities along X-, Y-, and Z-axes, respectively, ft/sec |
| $p, q, r$ | angular velocities about X-, Y-, and Z-axes, respectively, radians/sec |
| $\theta$ | angle of elevation of X body axis above a plane parallel to the x,z plane, radians |
| $\psi$ | angle in a plane parallel to the x,z plane between projection of the X body axis and an axis parallel to the X-axis, radians |
| $m$ | mass of body, slugs |
| $I_X, I_Y, I_Z$ | moment of inertia about X-, Y-, and Z-axes, respectively, slug-ft2 |
| $\mu$ | relative density factor, $m/\rho Sd$ |
| $\tau$ | nondimensional unit of time, $tV/d$ |
| $t$ | time, sec |
| $\rho$ | mass density of air, slugs/cu ft |
| $Q$ | dynamic pressure, lb/sq ft |
| $V$ | velocity of body, ft/sec |
| $M$ | Mach number, $V/a$ |
| $a$ | speed of sound in air, ft/sec |
| $S$ | body cross-sectional area, sq ft |
| $d$ | diameter of body, ft |
| $K_X^2, K_Y^2$ | nondimensional radii of gyration, $I_X/md^2$, $I_Y/md^2$ |
| $g$ | acceleration due to gravity, ft/sec |
| $P$ | period, sec |

$T_{1/2}$      time to **damp** to half-amplitude, sec

$D$      differential operator

$C_X$      force coefficient along X-axis,   $F_X/QS$

$C_Z$      force coefficient along Z-axis,   $F_Z/QS$

$C_Y$      force coefficient along Y-axis,   $F_Y/QS$

$C_m$      mcment coefficient about Y-axis,   $M_Y/QSd$

$C_n$      moment coefficient about Z-axis,   $M_Z/QSd$

$F_X$      force along X-axis

$F_Y$      force along Y-axis

$F_Z$      force along Z-axis

$M_X$      moment about X-axis

$M_Y$      moment about Y-axis

$M_Z$      moment about Z-axis

$$C_{X_\alpha} = \frac{\partial C_X}{\partial \alpha}$$

$$C_{Z_\beta} = \frac{\partial C_Z}{\partial \beta}$$

$$C_{X_r} = \frac{\partial C_X}{\partial \frac{rd}{2V}}$$

$$C_{Z_q} = \frac{\partial C_Z}{\partial \frac{qd}{2V}}$$

$$C_{m_\beta} = \frac{\partial C_m}{\partial \beta}$$

$$C_{m_q} = \frac{\partial C_m}{\partial \frac{qd}{2V}}$$

$$C_{n_{\dot{\alpha}}} = \frac{\partial C_n}{\partial \dot{\alpha}}$$

$$C_{n_r} = \frac{\partial C_n}{\partial \frac{rd}{2v}}$$

$\alpha$        angle of attack, $\tan^{-1} \dfrac{u}{\sqrt{v^2 + w^2}}$

$\gamma$        flight-path angle, positive up

$\beta = \tan^{-1} \dfrac{w}{v}$

Subscript:

o        initial conditions

     Bars over symbols indicate nondimensionalized factors. Dots over symbols indicate partial derivatives with respect to time.

<div align="center">CALCULATIONS</div>

<div align="center">Nonlinear</div>

     A series of calculations of the motion of spinning disk reentry bodies were made on an IBM type 704 electronic data processing machine for the spin rates and other conditions given in table I. Five degrees of freedom were employed in this work. These calculations were made, except as noted, for disks A and B having the cross-sectional shapes shown in figure 2. The aerodynamic and mass characteristics and initial conditions used in these calculations and referred to in table I are given in tables II, III, and IV, respectively. Newtonian aerodynamics were used to establish the stability derivatives. The equations of motion employed in these calculations are given in appendix A.

     A single calculation of the motion during reentry of a hypothetical statically stable ballistic missile (shape C of fig. 2) was made for comparison with the spinning disk shapes. The conditions for this calculation are given in tables I and V.

## Linear

A series of calculations of the roots of the linearized equations of motion of spinning disks (shapes A and B of fig. 2) were made to aid in understanding the results of the nonlinear calculations. In these calculations the spin rate, geometry, moments of inertia, and in some cases the aerodynamic derivatives were varied to determine the sensitivity of the motion to these factors. The results were expressed as periods and times to damp to half amplitude for the various modes of motion. The conditions for which these calculations were made are given in table VI along with the results. The aerodynamic derivatives and mass factors referred to in table VI are given in tables II and III except where otherwise noted. The linearized equations of motion are given in appendix B.

## RESULTS AND DISCUSSION

### Presentation of Results

The results of the investigation are presented in figures *3* to *6* and in table VI. The nonlinear reentry calculations are covered in the figures as plots of $a$, M, Q, $\psi$, t, z, and range plotted against altitude for various spin rates, two moments of inertia, and two configurations. The results of the linear calculations are given in table VI. Periods and times to damp to half amplitude are given for the four modes of motion. A comparison of certain linear calculations with corresponding nonlinear calculations is made in table VII.

### Discussion

An examination of the results of the reentry calculations for the spinning disks and a comparison with the statically stable ballistic missile (shape C) indicates that the behavior of the two is markedly different. (See figs. *3* to *6*.) The gyroscopic influence of the spinning disk combined with the aerodynamic static instability influences the motion in angle of attack to the extent that much greater angles of attack are experienced at 100,000 feet and below for the spinning disks than for the statically stable body. The spinning disks experience a continuing precessional motion about the wind vector throughout the flight as can be seen from the plots of $\psi$ against altitude. (See figs. 4 to 6.) The precessional rate is much greater for the less stable cases which pitch to relatively high angles of attack during reentry. (See figs. 4 and *5*.) These cases have smaller spin rates and hence less angular momentum with which to resist the unstable aerodynamic moment. As a result a greater precessional rate is required to obtain gyroscopic equilibrium.

A behavior in angle of attack which is of particular interest is evident for the thin disk body. (See fig. *5.)* In the case of the low spin rates, large angles of attack are developed from 120 to 30,000 feet. Below 30,000 feet the angles of attack are again comparable or less in magnitude to those at reentry. An examination of the Mach number history for these low spin rate cases indicates that there is an extremely rapid deceleration as the angle of attack becomes large (about 80g for calculation 10) followed by a region that more nearly approaches constant velocity near the ground. (See fig. 5(b).) This effect is not evident for the more stable high-spin-rate cases. The two most stable cases for the thin disks encounter a severe heating experience in that they impact at a Mach number of 12 or greater. The more blunt disk form that has a higher minimum drag coefficient exhibits the behavior in angle of attack to a lesser extent than the thin form. (See figs. 4 and *5.)*

An interesting feature of the performance of the disk forms during reentry is the relatively large dispersion that occurs as a result of the lift capability. (See figs. 4 and *5.)* This effect is evident in both the range and lateral displacement. Much less lateral displacement is obtained for some cases than for others. This effect is associated with the orientation of the model in precession as reentry is made.

## Linear Calculations

The linear calculations lend support to the general behavior shown by the reentry calculations. (See table VI.) A comparison of the linear and nonlinear calculations as to stability at 50,000 feet is given for shapes A and B in table VII. The results for shape B agree well in the linear and nonlinear cases as to the $pd/2V$ for instability. Less good agreement is shown for shape A. It is evident from these cases that the existence of an abrupt increase in angle of attack at the lower altitudes is evidence of an approach to an unstable behavior as indicated by a negative root for an altitude of 50,000 feet.

An examination of the roots from the linear calculations shows that instability is caused by a single root for the cases investigated. A pair of complex roots changes to real roots, one of which is unstable. This mode of motion then is simple divergence in angle of attack caused by the large static instability at high dynamic pressures.

## CONCLUSIONS

An analysis of the dynamic stability of spinning disks^-during atmospheric reentry leads to the following conclusions:

1. High rates of deceleration may be obtained for reentering spinning disks as a result of the instability which occurs at high dynamic pressures for sufficiently low spin rates.

2. General agreement was obtained between linear and nonlinear calculations for the spin rates at which angle-of-attack divergence occurs.

3. Considerable dispersion in impact point resulted because of the lift capability of the disk forms.

Langley Research Center,
    National Aeronautics and Space Administration,
        Langley Field, Va., August 5, 1959.

APPENDIX A

EQUATIONS OF MOTION USED IN THE NONLINEAR CALCULATIONS

The equations employed in this portion of the analysis are in the form frequently employed in ballistics work. They may be derived by resolving the body axis equations of motion along the X-, Y-, and Z-axes shown in figure 1. These X-, Y-, and Z-axes are different from body axes in that the Z-axis is constrained to a plane parallel to the xz ground reference system plane, and in that the body is free to spin about the X-axis. The X-axis is always alined with the axis of symmetry of the body.

Consider a view of the axis system along the X-axis with the body axes $Y_b$ and $Z_b$ displaced from Y and Z by an angle $\phi$
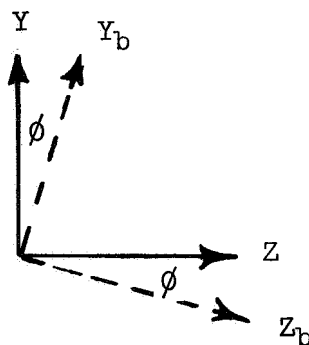


For the principal axes the equations of motion with respect to the body axes are:

$$
\left.
\begin{aligned}
F_{X,b} &= m\left(\dot{u}_b - r_b v_b + q_b w_b\right) \\
F_{Y,b} &= m\left(\dot{v}_b - p_b w_b + r_b u_b\right) \\
F_{Z,b} &= m\left(\dot{w}_b - q_b u_b + p_b v_b\right)
\end{aligned}
\right\} \tag{A1}
$$

$$
\left.
\begin{aligned}
M_{X,b} &= I_{X,b}\dot{p}_b - \left(I_{Y,b} - I_{Z,b}\right)q_b r_b \\
M_{Y,b} &= I_{Y,b}\dot{q}_b - \left(I_{Z,b} - I_{X,b}\right)r_b p_b \\
M_{Z,b} &= I_{Z,b}\dot{r}_b - \left(I_{X,b} - I_{Y,b}\right)p_b q_b
\end{aligned}
\right\} \tag{A2}
$$

where $F_X$, $F_Y$, and $F_Z$; $M_X$, $M_Y$, and $M_Z$; u, v, and w; p, q, and r; and $I_X$, $I_Y$, and $I_Z$ are the forces, moments, linear velocities, angular velocities, and moments of inertia for the X-, Y-, and Z-axes.

Expressing the components of these equations in terms of the XYZ system gives

$$\left.\begin{aligned}
F_{X,b} &= F_X \\
F_{Y,b} &= F_Y \cos\phi + F_Z \sin\phi \\
F_{Z,b} &= -F_Y \sin\phi + F_Z \cos\phi
\end{aligned}\right\} \tag{A3}$$

$$\left.\begin{aligned}
u_b &= u \\
v_b &= v \cos\phi + w \sin\phi \\
w_b &= -v \sin\phi + w \cos\phi
\end{aligned}\right\} \tag{A4}$$

$$\left.\begin{aligned}
M_{X,b} &= M_X \\
M_{Y,b} &= M_Y \cos\phi + M_Z \sin\phi \\
M_{Z,b} &= -M_Y \sin\phi + M_Z \cos\phi
\end{aligned}\right\} \tag{A5}$$

$$\left.\begin{aligned}
p_b &= p \\
q_b &= q \cos\phi + r \sin\phi \\
r_b &= -q \sin\phi + r \cos\phi
\end{aligned}\right\} \tag{A6}$$

$$\left.\begin{aligned}
I_{X,b} &= I_X \\
I_{Y,b} &= I_Y \\
I_{Z,b} &= I_Z
\end{aligned}\right\} \tag{A7}$$

Substituting these expressions into the body-axes equations of motion, grouping the sine and cosine parts, and assuming rotational symmetry where $I_Z = I_Y$ gives

$$M_X - I_X \dot{p} = 0$$

$$\left[ M_Z - I_Y(\dot{r} - q\dot{\phi}) - \left(I_Y - I_X\right)qp \right] \sin \phi + \left[ M_Y - I_Y(\dot{q} + r\dot{\phi}) \right.$$

$$\left. + \left(I_Y - I_X\right)rp \right] \cos \phi = 0$$

$$\left[ -M_Y + I_Y(\dot{q} + r\dot{\phi}) - \left(I_Y - I_X\right)rp \right] \sin \phi + \left[ M_Z - I_Y(\dot{r} + q\dot{\phi}) \right.$$

$$\left. - \left(I_Y - I_X\right)qp \right] \cos \phi = 0$$

$$\left. \right\} \quad \text{(A8)}$$

$$F_X - m(\dot{u} - rv + qw) = 0$$

$$\left[ F_Z - m(\dot{w} + v\dot{\phi} + pv - qu) \right] \sin \phi + \left[ F_Y - m(\dot{v} + w\dot{\phi} - pw + ru) \right] \cos \phi = 0$$

$$\left[ -F_Y - m(-\dot{v} - w\dot{\phi} + pw - ru) \right] \sin \phi + \left[ F_Z - m(\dot{w} - v\dot{\phi} + pv - qu) \right] \cos \phi = 0$$

$$\left. \right\}$$

$$\text{(A9)}$$

Making the kinematic substitution $\dot{\phi} = p - q \tan \theta$, equating the coefficients of the sine and cosine terms to zero which must be the case in order to satisfy each equation, and making appropriate selection of the force and moment terms in terms of gravity and aerodynamics gives the complete equations of motion. The $M_X$ equation goes to zero for constant spin rate **p** which is the case of interest for this **problem.**

The force equations are as follows:

X-force :

$$m(\dot{u} - rv + qw) - mg \cos \psi \cos \theta - QS\left(C_{X_\alpha}\alpha + C_{X_r} \frac{rd}{2V}\right) = 0 \qquad \text{(A10)}$$

Y-force :

$$m(\dot{v} - qv \tan \theta + ru) + mg \cos \psi \sin \theta - QSC_Y = 0 \qquad \text{(A11)}$$

Z-force :

$$m(\dot{w} - qu + qv \tan \theta) + mg \sin \psi - QS\left(C_{Z_\beta} \frac{w}{v} + C_{Z_q} \frac{qd}{2V}\right) = 0 \qquad \text{(A12)}$$

The moment equations are as **follows:**

Y-moment:

$$I_Y\dot{q} + r\left(I_X p - I_Y q \tan\theta\right) - QSd\left(-C_{n_\alpha}\alpha \sin\tan^{-1}\frac{V}{} - C_{m_q}\frac{qd}{2V}\right) = 0 \qquad (A13)$$

Z-moment:

$$I_Y\dot{r} - q\left(I_X p - qI_Y \tan\theta\right) - QSd\left(C_{n_\alpha}\alpha \cos\tan^{-1}\frac{w}{v} + C_{n_r}\frac{rd}{2V}\right) = 0 \qquad (A14)$$

where the following kinematic relations hold

$$\begin{aligned}
\dot{\theta} &= r \\
\dot{\psi} &= \frac{-q}{\cos\theta} \\
\dot{x} &= u\cos\theta\cos\psi - v\sin\theta\cos\psi - w\sin\psi \\
\dot{y} &= u\sin\theta + v\cos\theta \\
\dot{z} &= u\cos\theta\sin\psi - v\sin\theta\sin\psi + w\cos\psi \\
V &= \sqrt{u^2 + v^2 + w^2} \\
\alpha &= \tan^{-1}\frac{u}{\sqrt{v^2 + w^2}} \\
\beta &= \tan^{-1}\frac{w}{v} \\
Q &= \tfrac{1}{2}\rho V^2 = \tfrac{1}{2}\rho(u^2 + v^2 + w^2) \\
\rho &= f(x)
\end{aligned} \qquad (A15)$$

APPENDIX  B

EQUATIONS OF MOTION USED IN THE LINEAR CALCULATIONS

The force and moment equations for small disturbances are:

X-force:

$$m\dot{u} - QS\left(C_{X_\alpha} \frac{u}{V} + C_{X_r} \frac{rd}{2V}\right) - mrV = 0 \tag{B1}$$

Y-force:

$$m\dot{v} + \rho VvSC_Y + mg\theta = 0 \tag{B2}$$

Z-force:

$$m\dot{w} - QS\left(C_{Z_\beta} \frac{w}{V} + C_{Z_q} \frac{qd}{2V}\right) + mg\psi = 0 \tag{B3}$$

Y-moment:

$$I_Y\dot{q} - QSd\left(C_{m_\beta} \frac{w}{V} + C_{m_q} \frac{qd}{2V}\right) + rI_X p = 0 \tag{B4}$$

Z-moment:

$$I_Y\dot{r} - QSd\left(C_{n_\alpha} \frac{u}{V} + C_{n_r} \frac{rd}{2V}\right) - qI_X p = 0 \tag{B5}$$

By using the following relationships in equations (B1) to (B5)

$$\bar{p} = \frac{pd}{2V} \qquad q = \frac{qd}{2V} \qquad \bar{r} = \frac{rd}{2V}$$

$$\bar{\alpha} = \frac{u}{V} \qquad \bar{v} = \frac{v}{V} \qquad \bar{\beta} = \frac{w}{V}$$

$$\dot{\bar{\alpha}} = \frac{\partial \bar{\alpha}}{\partial \tau} \qquad \dot{\bar{v}} = \frac{\partial \bar{v}}{\partial \tau} \qquad \dot{\bar{\beta}} = \frac{\partial \bar{\beta}}{\partial \tau}$$

$$\dot{\theta} = \frac{\partial \theta}{\partial \tau} = 2\bar{r} \qquad \dot{\bar{\psi}} = \frac{\partial \psi}{\partial \tau} = -2\bar{q}$$

$$\ddot{\bar{\theta}} = \frac{\partial \dot{\bar{\theta}}}{\partial \tau} \qquad \ddot{\bar{\psi}} = \frac{\partial \dot{\bar{\psi}}}{\partial \tau}$$

$$\mu = \frac{m}{\rho S d}$$

$$K_X^2 = \frac{I_X}{md^2} \qquad K_Y^2 = \frac{I_Y}{md^2}$$

the nondimensionalized equations of motion are obtained as

$$2\mu\bar{\dot{\alpha}} - C_{X_\alpha}\bar{\alpha} - C_{X_r}\frac{\bar{\dot{\theta}}}{2} - 2\mu\bar{\theta} = 0 \qquad\qquad (B6)$$

$$\mu\bar{\dot{v}} - C_Y\bar{v} + \frac{C_X}{2}\theta = 0 \qquad\qquad (B7)$$

$$2\mu\bar{\dot{\beta}} - C_{Z_\beta}\bar{\beta} + \frac{C_{Z_q}}{2}\bar{\dot{\psi}} + C_X\psi = 0 \qquad\qquad (B8)$$

$$-2\mu K_Y^2\bar{\ddot{\psi}} - C_{m_\beta}\bar{\beta} + \frac{C_{m_q}}{2}\bar{\dot{\psi}} + 4\mu K_X^2\bar{\dot{\theta}}\bar{p} = 0 \qquad\qquad (B9)$$

$$2\mu K_Y^2\bar{\ddot{\theta}} - C_{n_\alpha}\bar{\alpha} - \frac{C_{n_r}}{2}\bar{\dot{\theta}} + 4\mu K_X^2\bar{\dot{\psi}}\bar{p} = 0 \qquad\qquad (B10)$$

Solving equations (B6) to (B10) simultaneously yields

$$A_1 D^6 + A_2 D^5 + A_3 D^4 + A_4 D^3 + A_5 D^2 + A_6 D + A_7 = 0$$

where $D = \frac{d}{d\tau}$ and $A_1$ to $A_7$ are the coefficients of the characteristic equation given by

$$A_1 = -16\mu^5 K_Y^4$$

$$A_2 = 4\mu^4 K_Y^2\left[2K_Y^2\left(C_{X_\alpha} + C_{Z_\beta} + 2C_Y\right) + C_{n_r} + C_{m_q}\right]$$

$$A_3 = 2\mu^3 K_Y^2\left\{2C_{n_\alpha}\left(\frac{C_{X_r}}{2} + 2\mu\right) - C_{X_\alpha}\left[2K_Y^2\left(C_{Z_\beta} + 2C_Y\right)\right.\right.$$

$$\left.+ C_{m_q} + C_{n_r}\right] - 2C_Y\left(2K_Y^2 C_{Z_\beta} + C_{m_q} + C_{n_r}\right)$$

$$\left. - C_{Z_\beta}\left(C_{n_r} + C_{m_q}\right) + C_{m_\beta}C_{Z_q}\right\} - \mu^3\left(C_{m_q}C_{n_r} + 64\mu^2 K_X^4\bar{p}^2\right)$$

$$A_4 = \mu^2 K_Y^2 \left\{ 2c_Y \left[ c_{Z_\beta}\left(2K_Y^2 c_{X_\alpha} + c_{n_r} + c_{m_q}\right) + c_{X_\alpha}\left(c_{n_r} + c_{m_q}\right) \right. \right.$$

$$\left. - c_{n_\alpha}\left(c_{X_r} + 4\mu\right) - c_{m_\beta}c_{Z_q} \right] + c_{Z_\beta}\left[ c_{X_\alpha}\left(c_{n_r} + c_{m_q}\right) - 2c_{n_\alpha}\left(\frac{c_{X_r}}{2} + 2\mu\right) \right]$$

$$\left. + c_{m_\beta}\left(4\mu c_X - c_{Z_q}c_{X_\alpha}\right) \right\} + \mu^2 c_{m_q}\left[ c_{n_r}\left(\frac{1}{2}c_{Z_\beta} + \frac{1}{2}c_{X_\alpha} + c_Y\right) \right.$$

$$\left. - c_{n_\alpha}\left(\frac{c_{X_r}}{2} + 2\mu\right) \right] + 32\mu^4 K_X^4 \bar{p}^2 \left(c_{X_\alpha} + c_{Z_\beta} + 2c_Y\right) - \frac{1}{2}\mu^2 c_{m_\beta}c_{Z_q}c_{n_r}$$

$$A_5 = \mu K_Y^2 \left\{ c_Y \left[ c_{X_\alpha}\left(c_{m_\beta}c_{Z_q} - c_{Z_\beta}c_{n_r} - c_{Z_\beta}c_{m_q} \right. \right. \right.$$

$$\left. \left. + 2c_{Z_\beta}c_{n_\alpha}\left(2\mu + \frac{c_{X_r}}{2}\right) - 4\mu c_X c_{m_\beta} \right] - 2\mu c_X c_{X_\alpha}c_{m_\beta} \right\}$$

$$+ \mu c_{m_q}\left\{ c_{n_\alpha}\left[ c_Y\left(2\mu + \frac{c_{X_r}}{2}\right) + c_{Z_\beta}\left(\frac{1}{4}c_{X_r} + \mu\right) \right] \right.$$

$$\left. - \frac{1}{2}c_{n_r}\left[ c_Y\left(c_{X_\alpha} + c_{Z_\beta}\right) + \frac{1}{2}c_{Z_\beta}c_{X_\alpha} \right] \right\}$$

$$+ \mu c_{m_\beta}\left\{ c_{Z_q}\left[ \frac{1}{2}c_{n_r}\left(\frac{1}{2}c_{X_\alpha} + c_Y\right) - c_{n_\alpha}\left(\mu + \frac{1}{4}c_{X_r}\right) \right] - \mu c_X c_{n_r} \right\}$$

$$- 16\mu^3 K_X^4 \bar{p}^2 \left[ 2c_Y\left(c_{X_\alpha} + c_{Z_\beta}\right) + c_{Z_\beta}c_{X_\alpha} \right]$$

$$A_6 = \mu c_{m_\beta}\left\{ c_Y\left(c_{Z_q}c_{n_\alpha} + 2K_Y^2 c_X c_{X_\alpha} + c_X c_{n_r}\right) \right.$$

$$\left. + c_X\left[ \frac{1}{2}c_{n_r}c_{X_\alpha} - c_{n_\alpha}\left(\frac{c_{X_r}}{2} + 2\mu\right) \right] \right\}$$

$$+ \mu c_{Z_\beta}\left[ c_Y\left(16\mu K_X^4 \bar{p}^2 c_{X_\alpha} - c_{m_q}c_{n_\alpha}\right) \right] + \frac{1}{2}c_Y\left[ c_{n_\alpha}\frac{c_{X_r}}{2}\left(c_{m_\beta}c_{Z_q} \right. \right.$$

$$\left. \left. - c_{m_q}c_{Z_\beta}\right) + \frac{1}{2}c_{n_r}c_{X_\alpha}\left(c_{m_q}c_{Z_\beta} - c_{m_\beta}c_{Z_q}\right) \right]$$

$$A_7 = c_{m_\beta}c_X c_Y\left[ c_{n_\alpha}\left(2\mu + \frac{c_{X_r}}{2}\right) - \frac{1}{2}c_{n_r}c_{X_\alpha} \right]$$
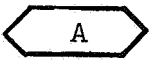
TABLE I

CONDITIONS FOR THE NONLINEAR CALCULATIONS

| Calculation number | Spin rate, radians/sec | Aerodynamic derivatives see tables II and V) for configuration. | Inertial constants (see table III) | Initial conditions (see table IV) |
|---|---|---|---|---|
| 1 | 220 | A | E | G |
| 2 | 110 | A | E | G |
| 3 | 55 | A | E | G |
| 4 | 40 | A | E | G |
| 5 | 220 | A | D | G |
| 6 | 220 | B | E | G |
| 7 | 110 | B | E | G |
| 8 | 55 | B | E | G |
| 9 | 28 | B | E | G |
| 10 | 14 | B | E | G |
| 11 | 0 | C | * | H |

*
 Inertial constants are given in table V.

## TABLE II

### AERODYNAMIC DERIVATIVES USED IN THE CALCULATIONS

| | Configuration cross section A | Configuration cross section B |
|---|---|---|
| $c_{X_\alpha}$ · · · · · · | -0.50 | -0.95 |
| $c_{Z_\beta}$ · · · · · · | 0 | 0 |
| $c_Y$ · · · · · · | -0.25 | -0.03 |
| $c_{X_r}$ · · · · · · | 0.40 | 0.20 |
| $c_{Z_q}$ · · · · · · | 0 | 0 |
| $c_{m_\beta}$ · · · · · · | 0 | 0 |
| $c_{m_q}$ · · · · · · | -0.08 | -0.16 |
| $c_{n_\alpha}$ · · · · · · | 0.20 | 0.23 |
| $c_{n_r}$ · · · · · · | -0.20 | -0.10 |

TABLE III

MASS AND DIMENSIONAL CONSTANTS USED IN THE CALCULATIONS

| Constants | D | E |
|---|---|---|
| Mass, slugs . . . . . . . . . . . . | 100 | 100 |
| $I_X$, slugs-ft$^2$ . . . . . . . . . . . . | 230 | 378 |
| $I_Y$, slugs-ft$^2$ . . . . . . . . . . . . | 200 | 189 |
| S, sq ft . . . . . . . . . . . . . . | 24 | 24 |
| d, ft . . . . . . . . . . . . . . . | 5.5 | 5.5 |

TABLE IV

INITIAL CONDITIONS

| Condition | G | H |
|---|---|---|
| h, f t . . . . . . . . . . . . | 400,000 | 400,000 |
| $x_0$, f t . . . . . . . . . . . | -400,000 | -400,000 |
| $y_0$, f t . . . . . . . . . . | 0 | 0 |
| $z_0$, f t . . . . . . . . . . . | 0 | 0 |
| $\dot{x}_0$, ft/sec . . . . . . . . . . | 8,040 | 8,802 |
| $\dot{y}_0$, ft/sec . . . . . . . . . . | 19,420 | 21,249 |
| $\dot{z}_0$, ft/sec . . . . . . . . . . | 0 | 0 |
| $V_0$, ft/sec . . . . . . . . . | 21,000 | 23,000 |
| $\theta_0$, d e g . . . . . . . . . . . | -12.5 | -12.5 |
| $\psi_0$, d e g . . . . . . . . . . . | 0 | 0 |
| $\alpha_0$, d e g . . . . . . . . . . . . | 10.0 | 10.0 |
| $y$, deg . . . . . . . . . . . | -22.5 | -22.5 |

## TABLE V

### INERTIAL, CONSTANTS AND AERODYNAMIC DERIVATIVES

### FOR HYPOTHETICAL BALLISTIC **MISSILE** (SHAPE C)

| | |
|---|---|
| Mass, slugs . . . . . . . . . . . . . . . . . . . . . . . . . . . . . . | 106 |
| $I_X$, slug-ft2 . . . . . . . . . . . . . . . . . . . . . . . . . . . | 80 |
| $I_Y$, slug-ft$^2$ . . . . . . . . . . . . . . . . . . . . . . . . . . | 900 |
| $I_Z$, slug-ft2 . . . . . . . . . . . . . . . . . . . . . . . . . . . | 900 |
| S, sq ft . . . . . . . . . . . . . . . . . . . . . . . . . . | 6.1 |
| d, ft . . . . . . . . . . . . . . . . . . . . . . . . . . . | 2.79 |
| Axial-force coefficient . . . . . . . . . . . . . . . . . . . . | -0.542 |
| Normal-force-coefficient slope with angle of attack . . . . . | -4.00 |
| Pitching-moment-coefficient slope with angle of attack . . . | -0.565 |
| Pitch damping . . . . . . . . . . . . . . . . . . . . . . . . | 0 |

TABLE VI

RESULTS OF LINEAR CALCULATIONS

| ase | Derivatives for configurations | Mass factors See table III | pd 2V | μ | 1st mode P | 1st mode T₁/₂ | 2d mode P | 2d mode T₁/₂ | 3d mode P | 3d mode T₁/₂ | 4th mode P | 4th mode T₁/₂ |
|---|---|---|---|---|---|---|---|---|---|---|---|---|
| 1 | A | D | .032 | 2,100 | -------- | 3,545.74 | ------ | 3,299.14 | 53.02 | 1,568.25 | - | ------ |
| 2 | A | D | .016 | 2,100 | -------- | 4,423.65 | ------ | 3,364.72 | 143.51 | 1,500.72 | - | ------ |
| 3 | A | D | .014 | 2,100 | -------- | 3,050.0 | ------ | 3,280.0 | 203.48 | 1,423.61 | - | ------ |
| 4 | A | D | .012 | 2,100 | -------- | -1,289.84 | ------ | 3,342.97 | 557.36 | 8,573.89 | - | ------ |
| 5 | A | D | .010 | 2,100 | -------- | -29.385 | ------ | 3,362.46 | -------- | 1,867.42 | - 28.53 | |
| 6 | A | D | .008 | 2,100 | -------- | -20.72 | ------ | 3,362.74 | -------- | 2,400.66 | - 20.24 | |
| 7 | A | D | .004 | 2,100 | -------- | -16.01 | ------ | 3,362.28 | -------- | 2,710.91 | - 15.72 | |
| 8 | A | D | .002 | 2,100 | -------- | -15.26 | ------ | 3,362.47 | -------- | 2,759.38 | - 14.99 | |
| 9 | A | D | .001 | 2,100 | -------- | -15.09 | ------ | 3,362.47 | -------- | 2,770.42 | - 14.82 | |
| 10 | A | D | .000 | 2,100 | -------- | -15.05 | ------ | 3,361.77 | -------- | 2,773.59 | - 14.78 | |
| 11 | A | E | .032 | 2,100 | -------- | 2,855.88 | ------ | 4,156.50 | 28.99 | 1,499.12 | - | ------ |
| 12 | A | E | .016 | 2,100 | -------- | 3,260.32 | ------ | 3,716.73 | 62.84 | 1,479.94 | - | ------ |
| 13 | A | E | .008 | 2,100 | -------- | 3,362.46 | ------ | 18,088.55 | 224.16 | 1,270.22 | - | ------ |
| 14 | A | E | .004 | 2,100 | -------- | -17.99 | ------ | 3,362.56 | -------- | 2,318.91 | - 17.61 | |
| 15 | A | E | .002 | 2,100 | -------- | -15.30 | ------ | 3,362.36 | -------- | 2,575.32 | - 14.55 | |
| 16 | A | E | .001 | 2,100 | -------- | -14.79 | ------ | 3,363.27 | -------- | 2,614.16 | - 14.52 | |
| 17 | A | E | .000 | 2,100 | -------- | -14.67 | ------ | 3,363.07 | -------- | 2,623.53 | - 14.41 | |
| 18 | B | D | .032 | 2,100 | -------- | 28,514.7 | ------ | 1,860.2 | 53.43 | 1,669.2 | - | ------ |
| 19 | B | D | .016 | 2,100 | -------- | 28,049.7 | ------ | 3,123.9 | 157.9 | 1,412.3 | - | ------ |
| 20 | B | D | .008 | 2,100 | -------- | -18.23 | ------ | 28,018.0 | -------- | 1,206.4 | - 17.93 | |
| 21 | B | D | .004 | 2,100 | -------- | -14.77 | ------ | 28,019.9 | -------- | 1,353.7 | - 14.56 | |
| 22 | B | D | .002 | 2,100 | -------- | -14.18 | ------ | 28,018.0 | -------- | 1,379.2 | - 13.98 | |
| 23 | B | D | .001 | 2,100 | -------- | -14.04 | ------ | 28,010.1 | -------- | 1,385.1 | - 13.84 | |
| 24 | B | D | .000 | 2,100 | -------- | -14.01 | ------ | 28,018.0 | -------- | 1,386.5 | - 13.81 | |
| 25 | B | E | .032 | 2,100 | -------- | 1,763.6 | ------ | 44,154.2 | 28.60 | 1,632.7 | - | ------ |
| 26 | B | E | .016 | 2 100 | -------- | 1,953.8 | ------ | 28,166.6 | 63.72 | 1,556.1 | - | ------ |
| 27 | B | E | .008 | 2,la. | -------- | -1,721.1 | ------ | 28,022.2 | 298.33 | 833.57 | - | ------ |
| 28 | B | E | .004 | 2,100 | -------- | -16.20 | ------ | 28,016.0 | -------- | 1,187.1 | - 15.95 | |
| 29 | B | E | .002 | 2,100 | -------- | -14.15 | ------ | 28,021.9 | -------- | 1,287.3 | - 13.95 | |
| 30 | B | E | .001 | 2,100 | -------- | -13.75 | ------ | 28,023.8 | -------- | 1,307.2 | - 13.55 | |
| 31 | B | E | .000 | 2,100 | -------- | -13.65 | ------ | 28,018.0 | -------- | 1,311.9 | - 13.46 | |
| 32 | , ana $c_{n_r} = -5.1$ | E | .008 | 2,100 | -------- | 17,548.3 | ------ | 3,369.4 | 233.96 | 81.92 | - | ------ |
| 33 | , ana $c_{n_r} = -1.($ | E | .008 | 2,100 | -------- | 16,708.6 | ------ | 3,412.8 | 224.45 | 371.68 | - | ------ |
| 34 | ᴌ ana $c_{n_r} = 0$ | E | .008 | 2,100 | -------- | 18,066.9 | ------ | 3,363.7 | 224.22 | 3,210.5 | - | ------ |
| 35 | ᴌ ana $c_{n_r} = 0.2$ | E | .008 | 2,100 | -------- | 18,149.6 | ------ | 3,361.4 | 224.22 | -6,080.9 | - | ------ |
| 36 | , and $c_{n_r} = 1.0$ | E | .008 | 2,100 | -------- | 18,144.2 | ------ | 3,363.7 | 224.65 | -48,364 | - | ------ |
| 37 | ᴌ ana $c_{n_\alpha} = -0.$ | E | .008 | 2 100 | -------- | 2,943.7 | ------ | 3,440.9 | 85.86 | 1,542.2 | - | ------ |
| 38 | ᴌ ana $c_{n_\alpha} = 0$ | E | .008 | 2,100 | 549,871.9 | 3,362.9 | 113.40 | 1,501.0 | -------- | ----------- | - | ------ |
| 39 | ᴌ and $c_{n_\alpha} = 0.0$ | E | .008 | 2,100 | -------- | 3,372.9 | ------ | 3,524.1 | 122.86 | 1,485.5 | - | ------ |
| 40 | ᴌ and $c_{m_q} = -1.$ | E | .008 | 2,100 | -------- | -88.61 | ------ | 3,362.7 | 215.96 | 115.6( | - | ------ |
| 41 | ᴌ and $c_{m_q} = -0.$ | E | .008 | 2,100 | -------- | -233.52 | ------ | 3,360.6 | 222.76 | 269.0: | - | ------ |
| 42 | ᴌ and $c_{m_q} = 0$ | E | .008 | 2,100 | -------- | 816.43 | ------ | 3,330.0 | 224.15 | 23,001.5 | - | ------ |
| 43 | ᴌ ana $c_m = 0.0$ | E | .008 | 2,100 | -------- | 442.33 | ------ | 3,314.0 | 223.99 | -1,431.9 | - | ------ |
| 44 | ᴌ ana $c_{m_q} = 0.4$ | E | .008 | 2,100 | -------- | 153.40 | ------ | 3,361.4 | 222.01 | -278.8. | - | ------ |
| 45 | ᴌ ana $c_m = -5.$ | E | .008 | 2,100 | -------- | -31.32 | ------ | 3,362.5 | 175.34 | 35.1: | - | ------ |
| 46 | A | E | .008 | 318 | -------- | -.98ᴇ | ------ | 77.10 | -------- | 57.0: | - .933 | |
| 47 | A | E | .008 | 432 | -------- | -1.63 | ------ | 102.60 | -------- | 142.2ᴇ | - 1.55 | |
| 48 | A | E | .008 | 24,000 | -------- | 376,790.5 | ------ | 538,918.4 | 1,154.9 | 220,492.3 | - | ------ |
| 49 | A | E | .008 | ,350,000 | -------- | 13.89 x 10⁶ | ------ | 13.90 x 10 | 72,937.0 | 62.03 x 10' | - | ------ |

TABLE VII

COMPARISON OF STABILITY OF CASES CALCULATED BY NONLINEAR

METHODS WITH CASES CALCULATED BY LINEAR METHODS

| Calculation (See table I) | $\frac{pd}{2V}$ for 50,000 feet | Behavior below 50,000 feet | Calculation (See table VI) | $\frac{pd}{2V}$ for 50,000 feet | Root |
|---|---|---|---|---|---|
| Configuration A | | | Configuration A | | |
| 1 | 0.04426 | Stable | 11 | 0.032 | Stable |
| 2 | .02236 | Stable | 12 | .016 | Stable |
| 3 | .01138 | Unstable | 13 | .008 | Stable |
| 4 | .00868 | Unstable | 14 | .004 | Unstable |
| Configuration B | | | Configuration B | | |
| 6 | 0.03055 | Stable | 25 | 0.032 | Stable |
| 7 | .01531 | Stable | 26 | .016 | Stable |
| 8 | .00809 | Unstable | 27 | .008 | Unstable |
| 9 | .00678 | Unstable | 28 | .004 | Unstable |
| 10 | .00626 | Unstable | 29 | .002 | Unstable |
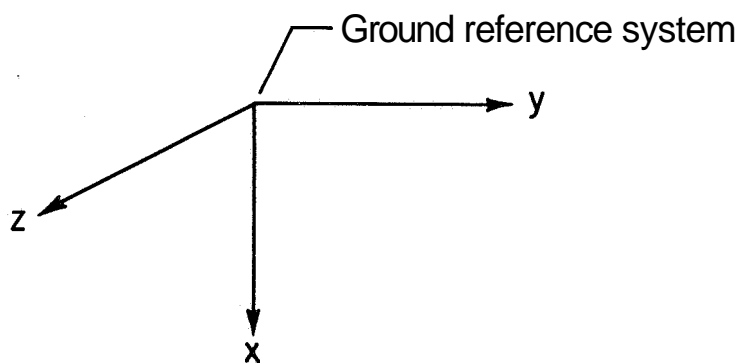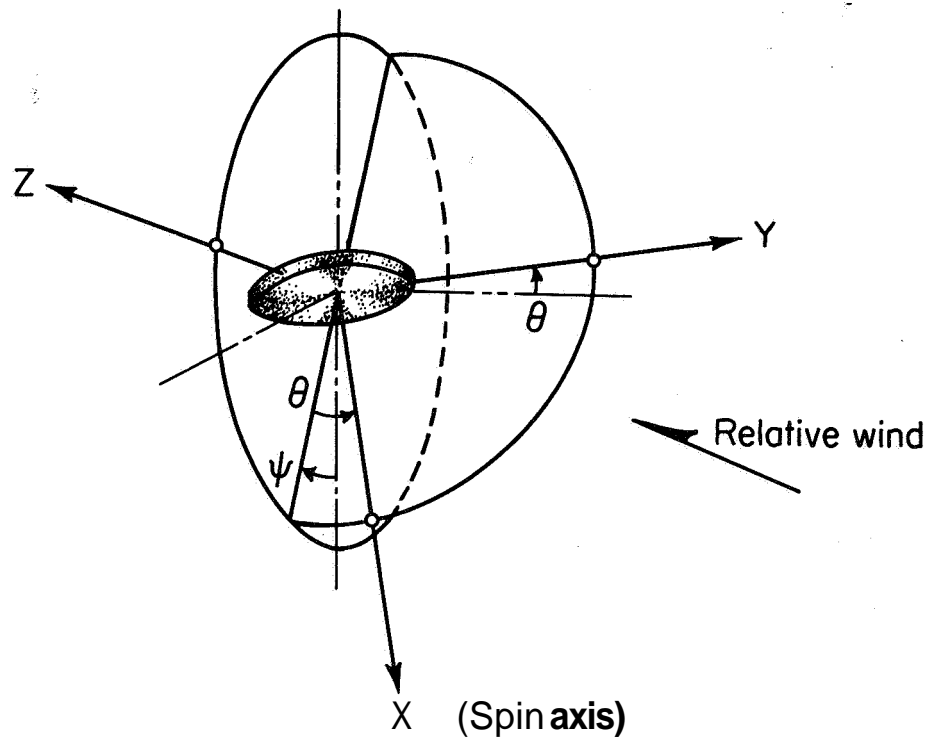
(a) Euler angles.

Figure 1.- Axis system used in calculations.
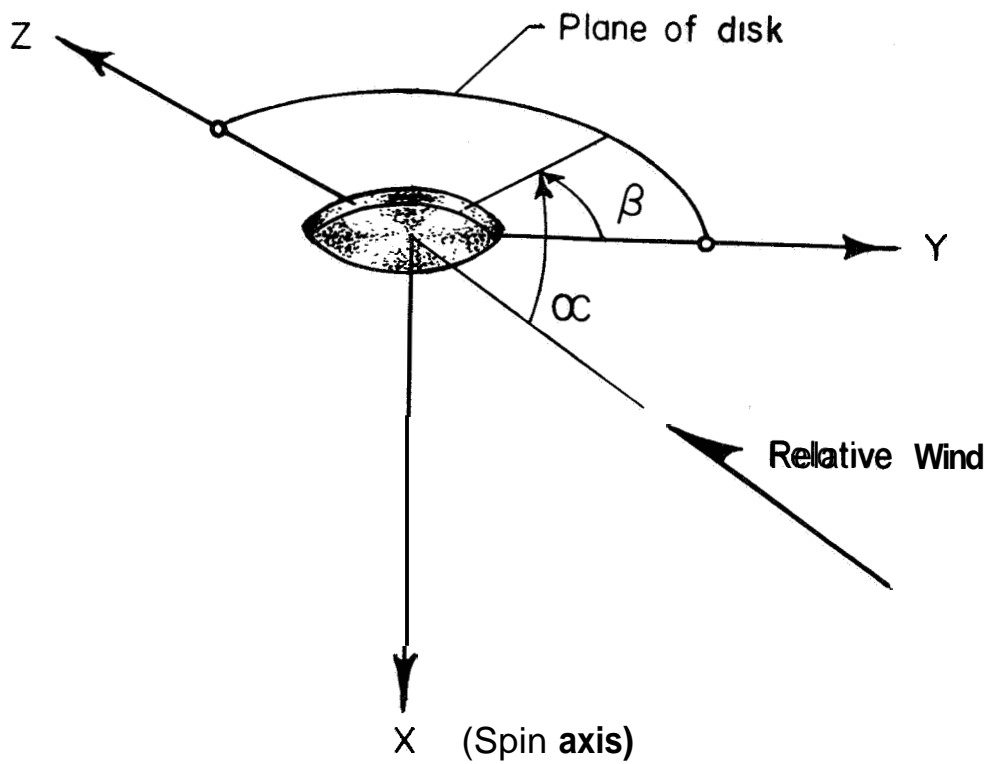
(b) Aerodynamic angles.

Figure 1.- Concluded.
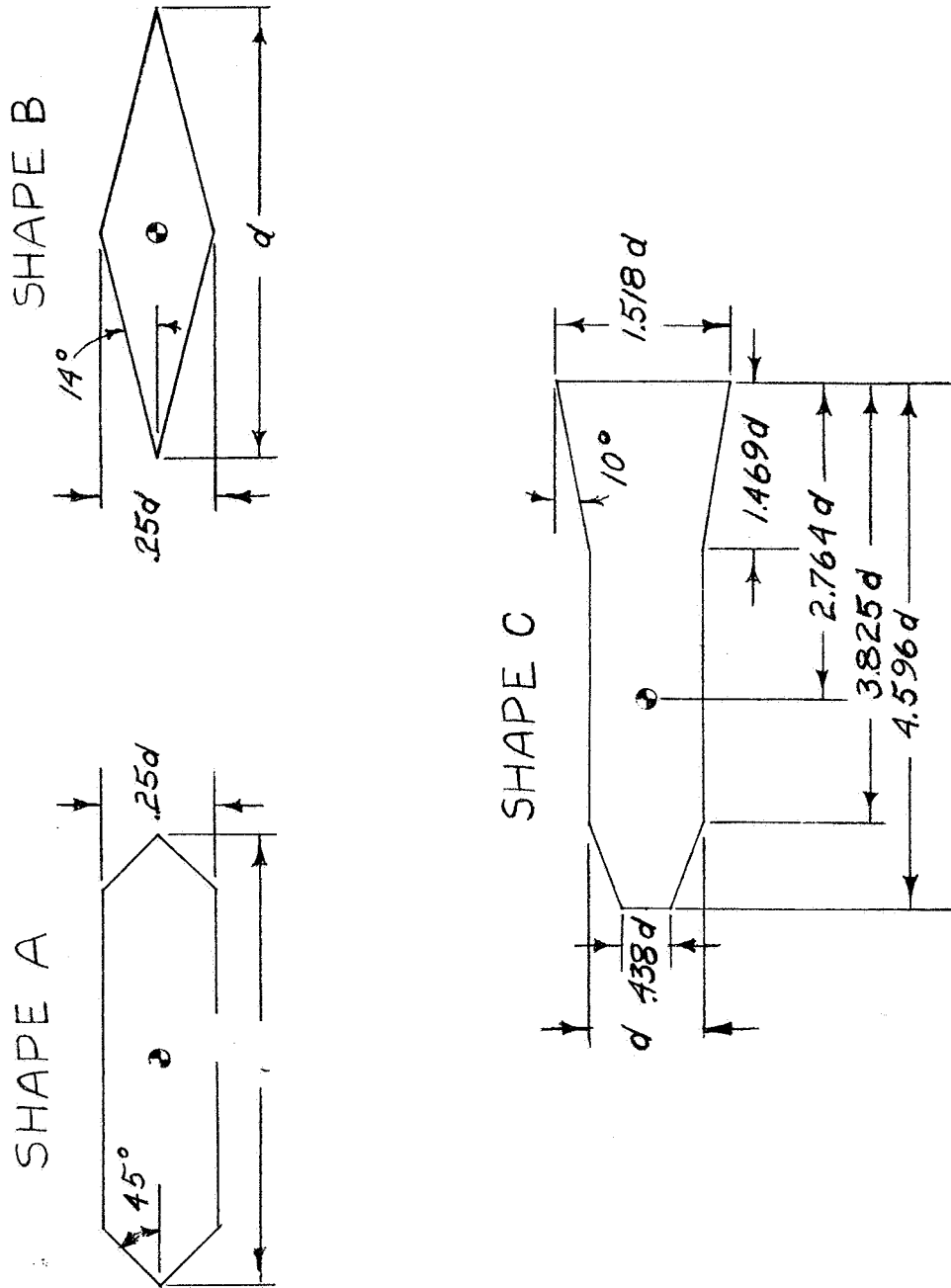
Figure 2.- Shapes used in the nonlinear and linear calculations.
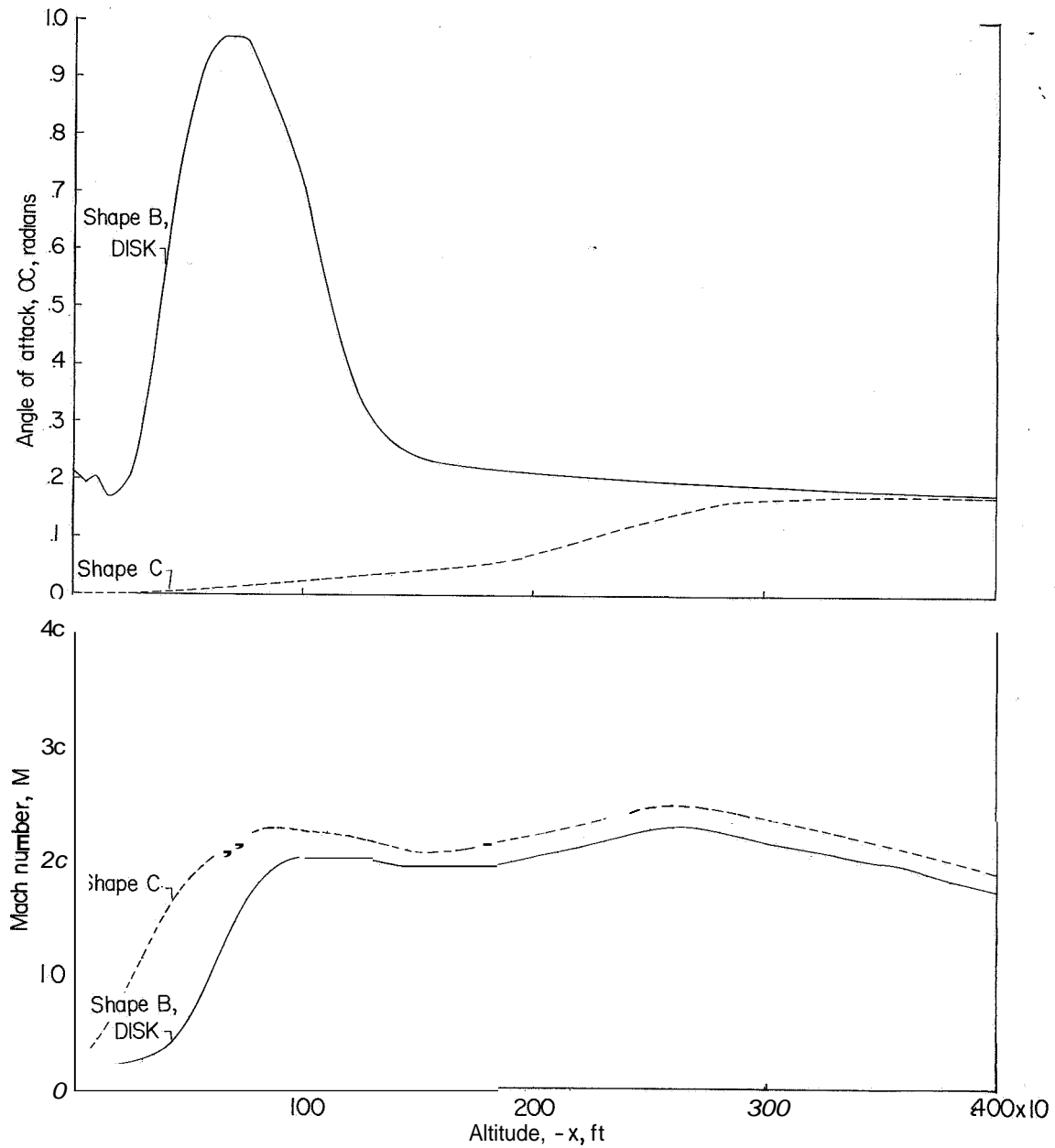
Figure *3.-* Comparison of the reentry behavior of shape B at 14 radians per second with that of shape C.
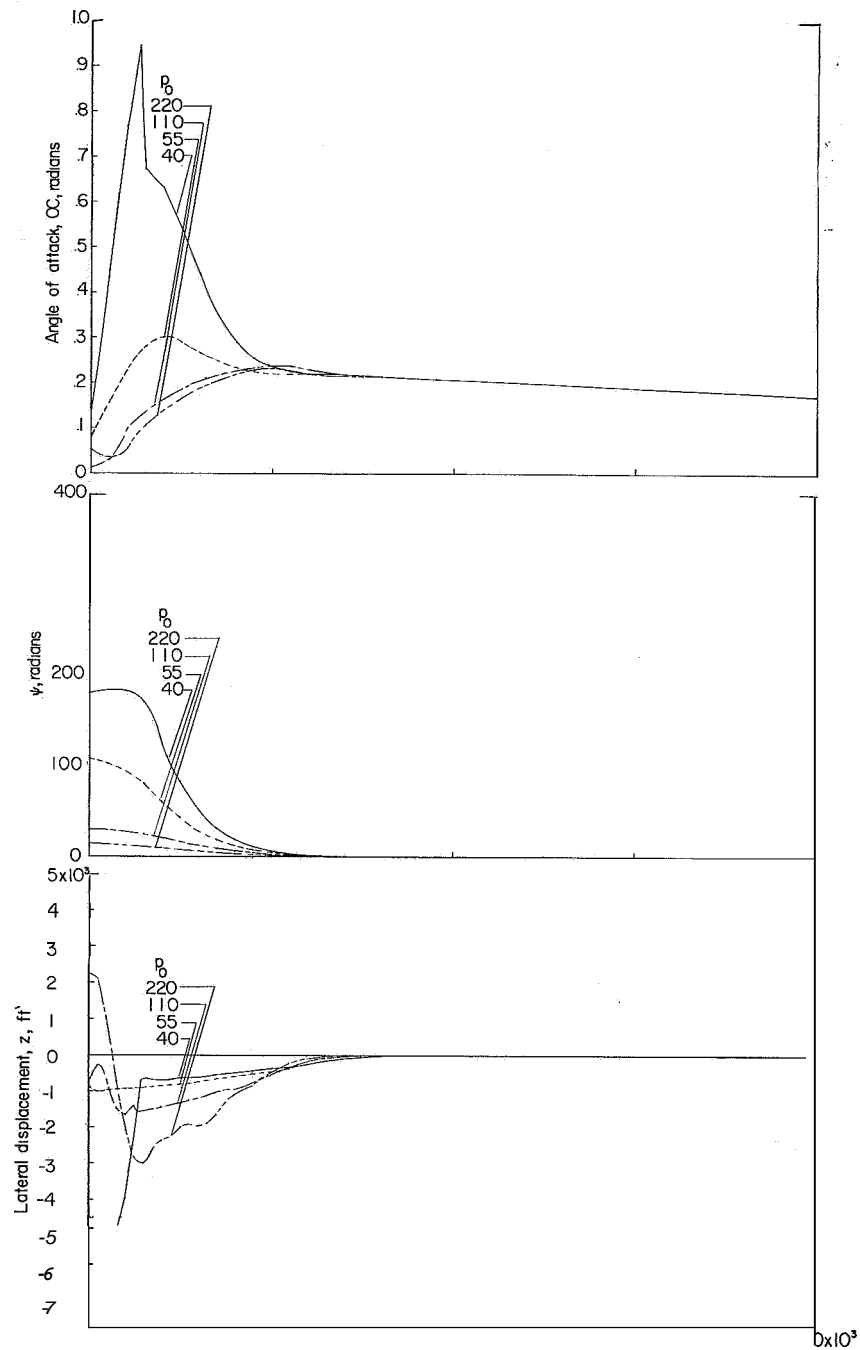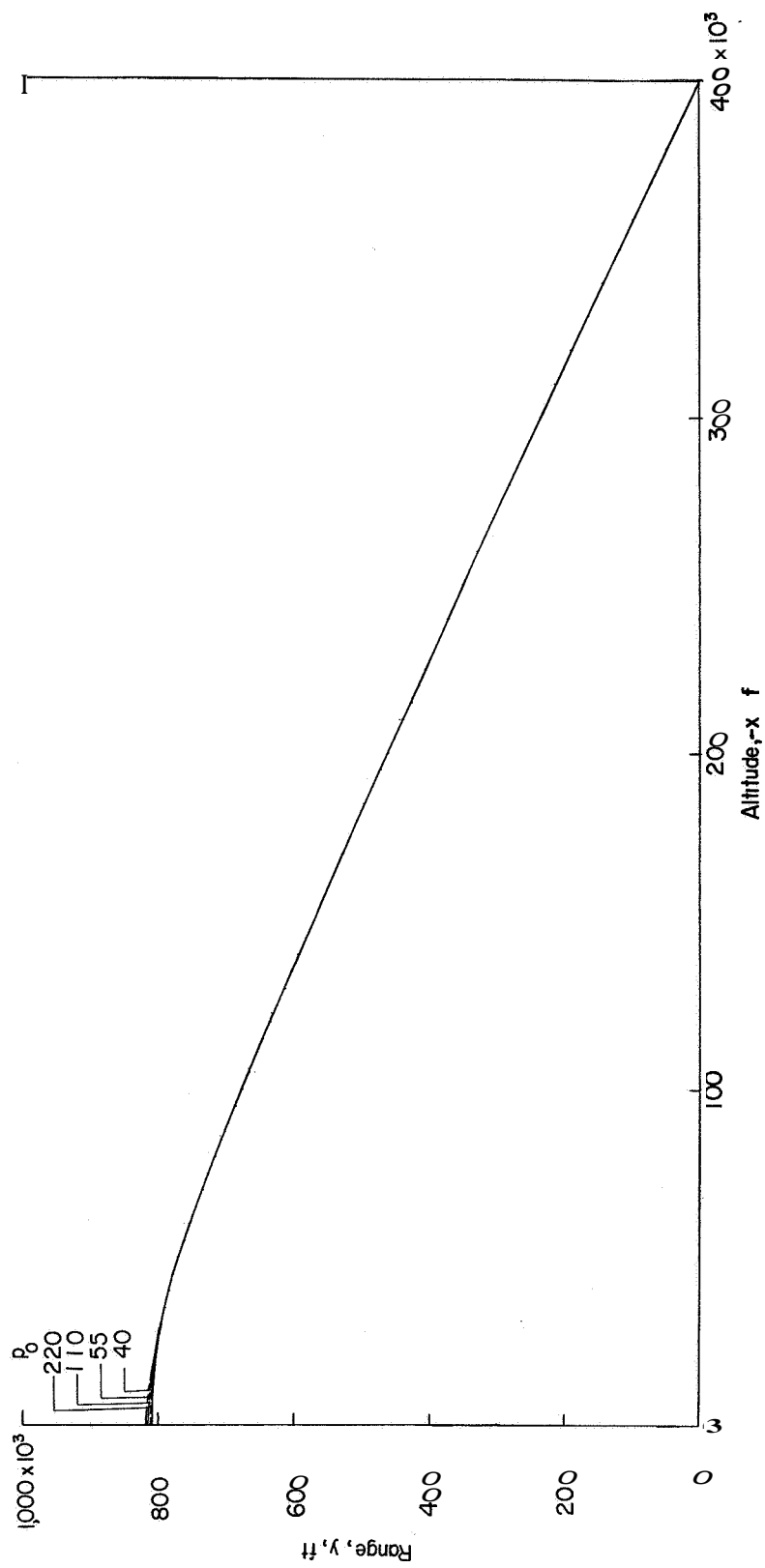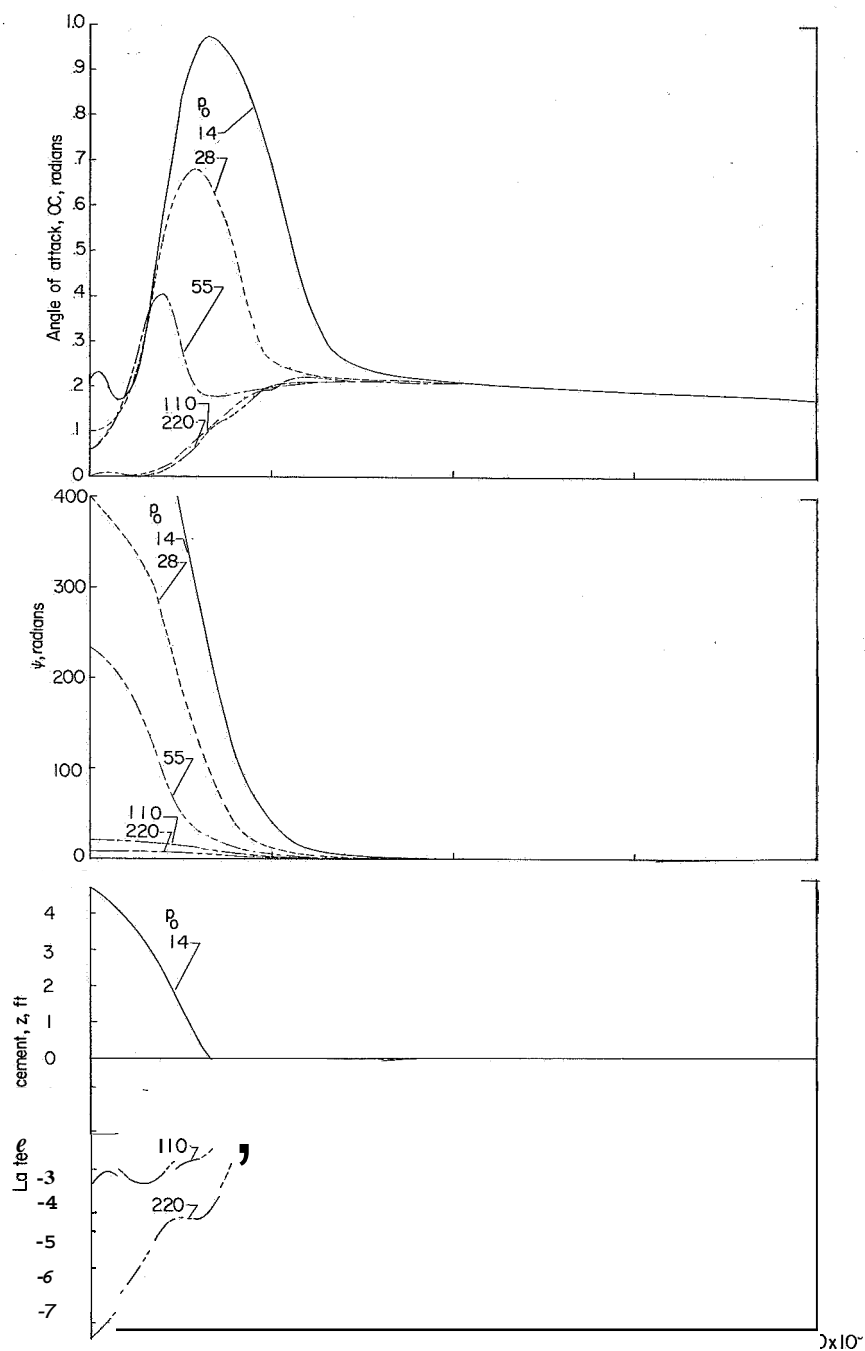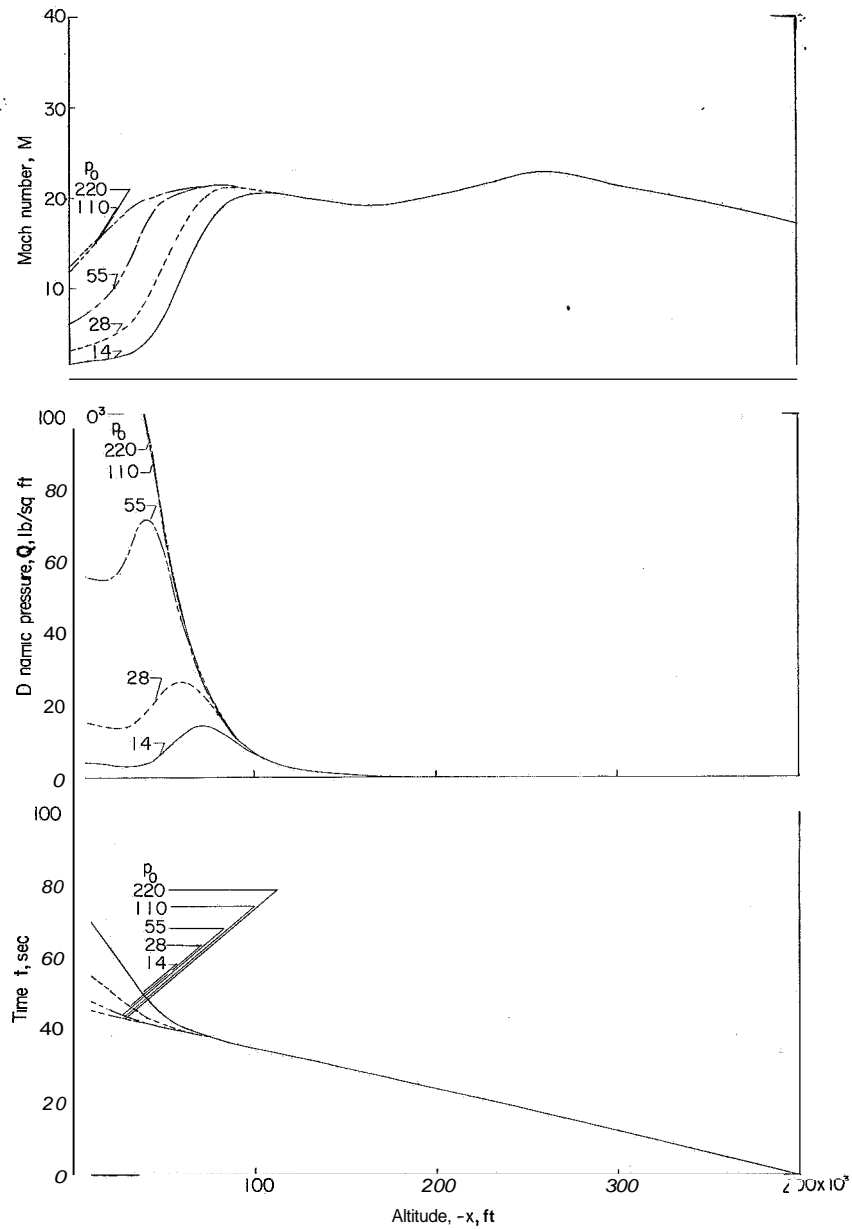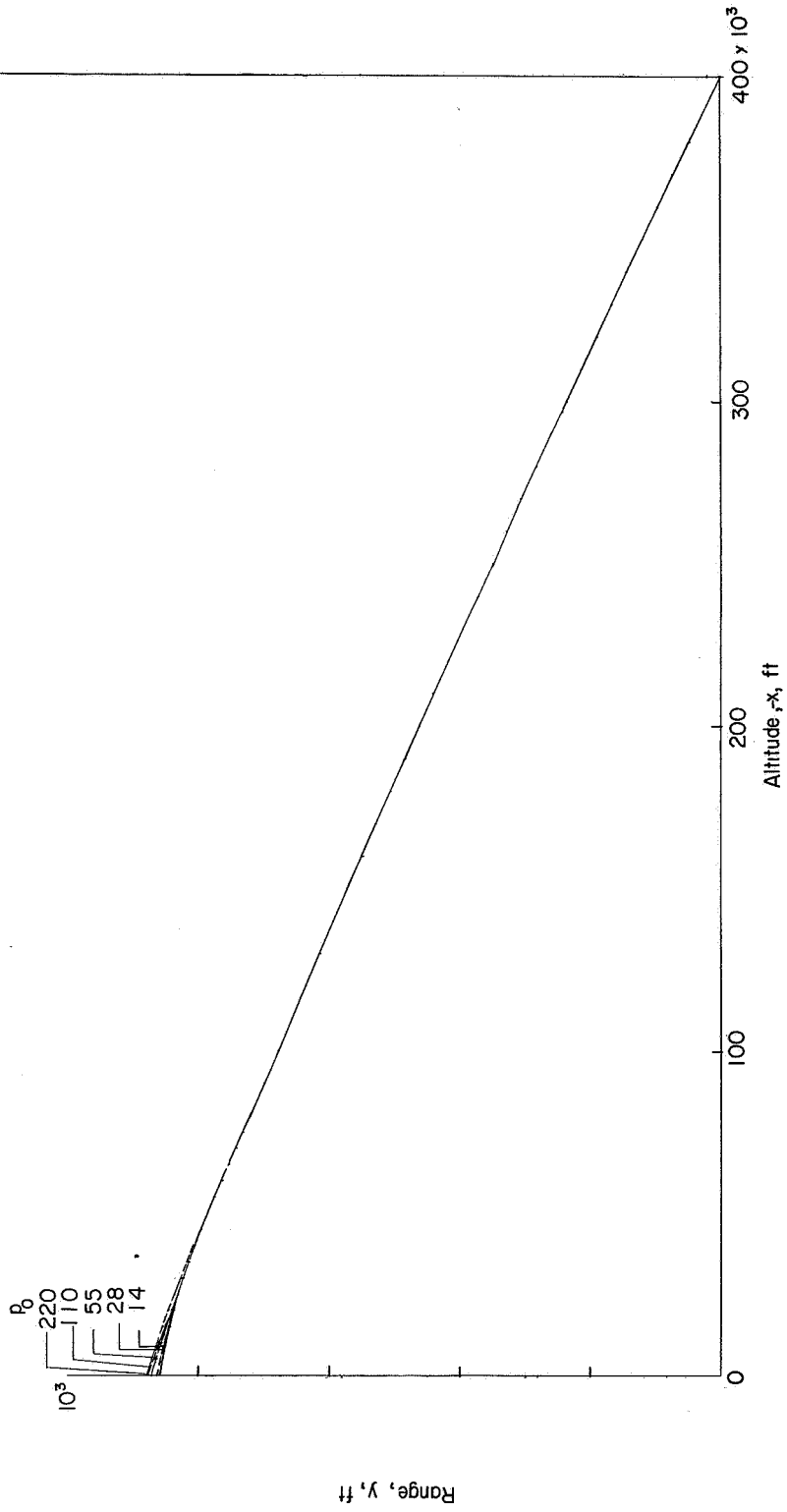
Figure 4.- Comparison of the reentry behavior of shape A for various spin rates. Calculations 1 to 4.
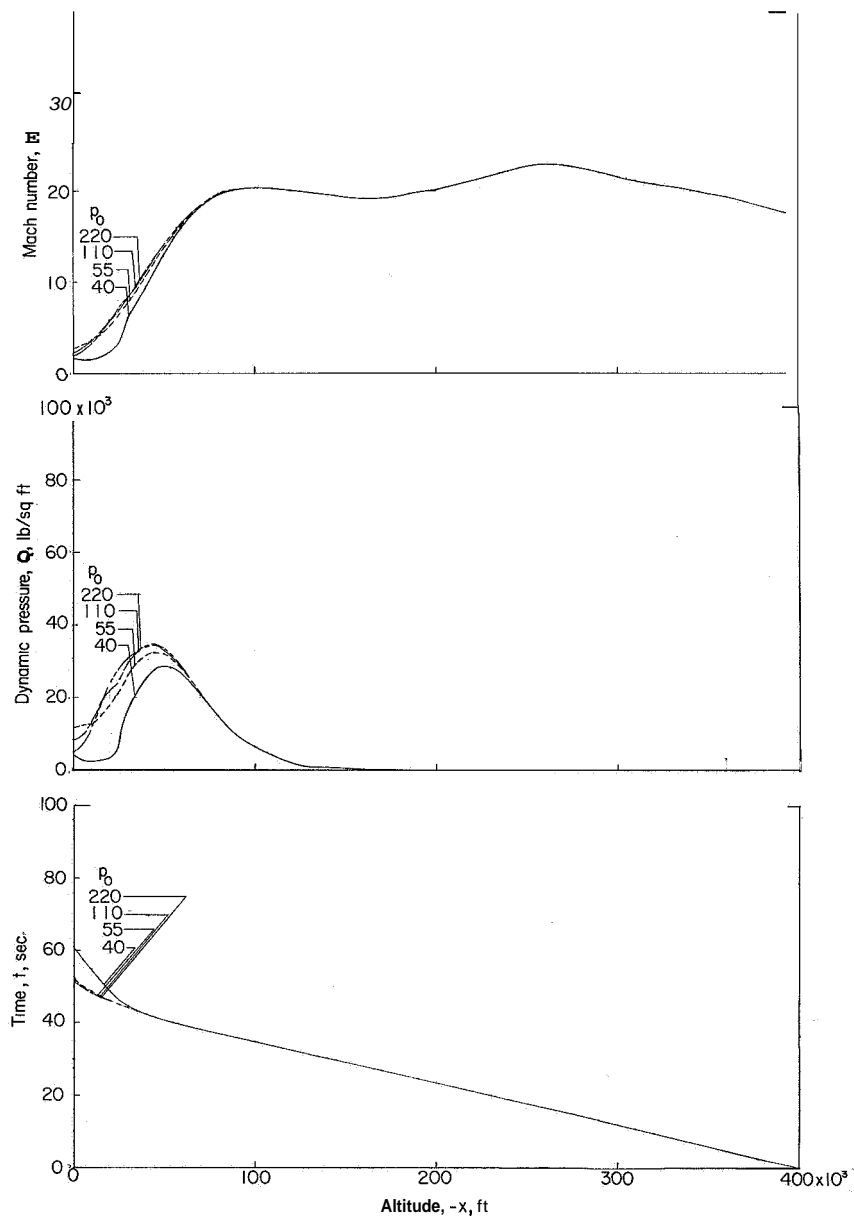
(b) Mach number, dynamic pressure, and time.

Figure 4.- Continued.

Altitude,-x f

(c) Range.

Figure 4.- Concluded.

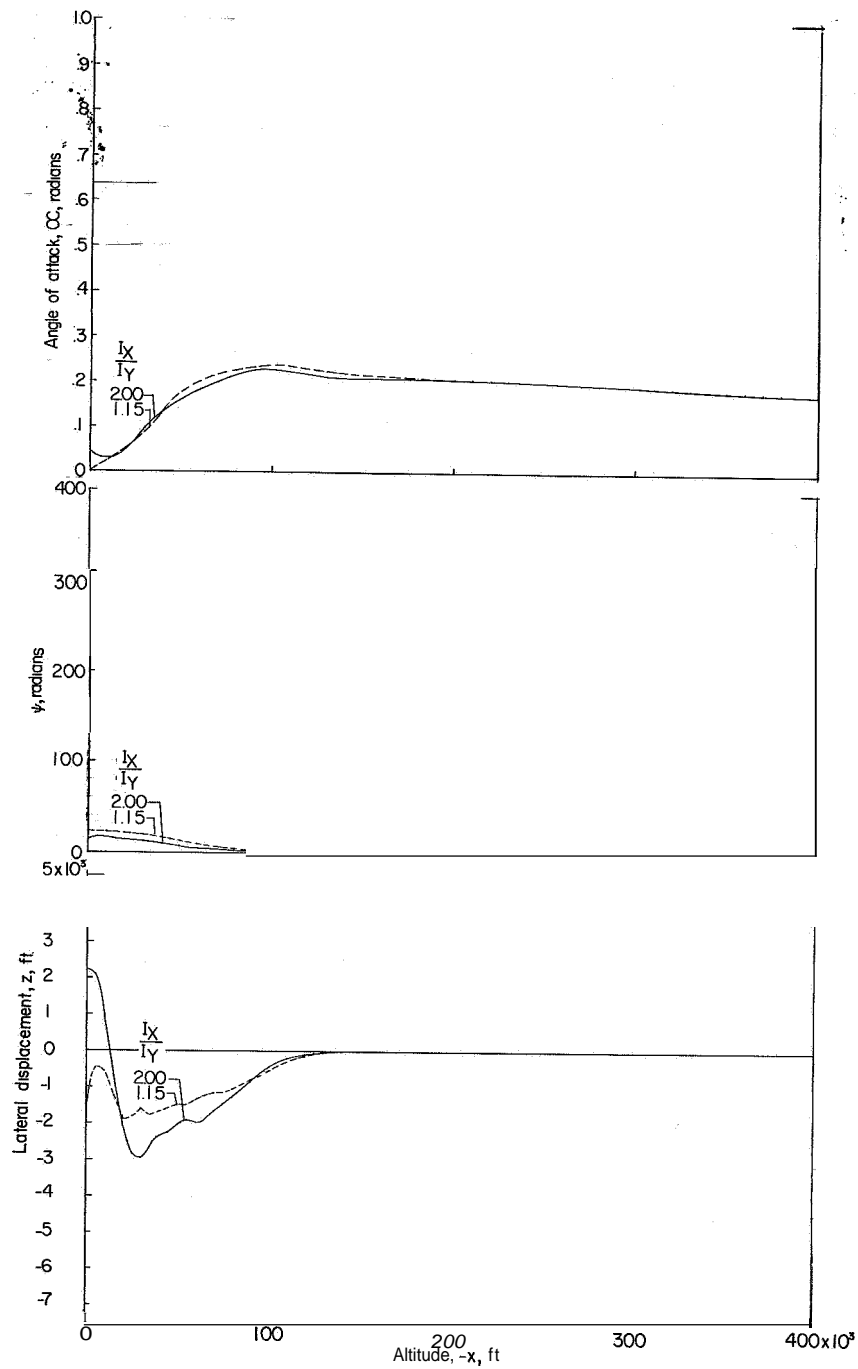Figure 5.- Comparison of the reentry behavior of shape B for various spin rates. Calculations 6 to 10.

(b) Mach number, dynamic pressure, and time.
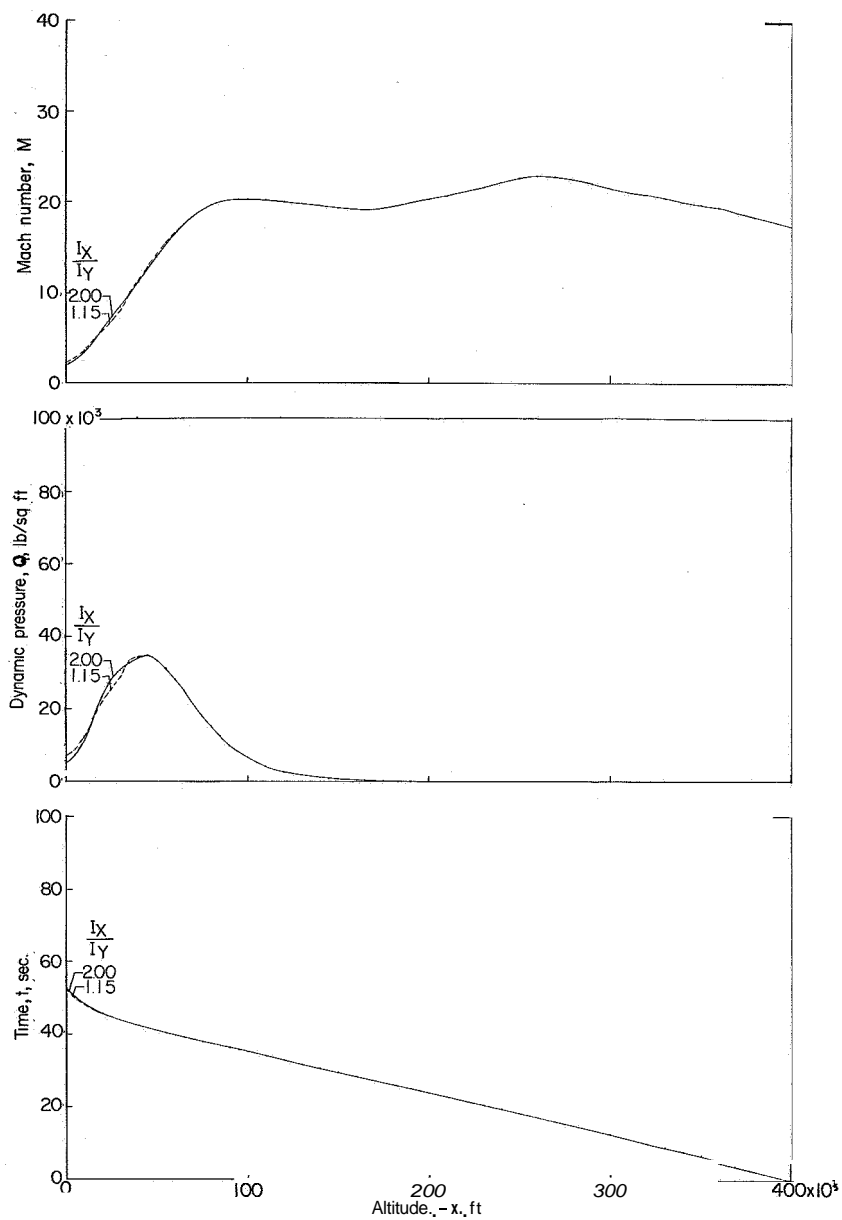
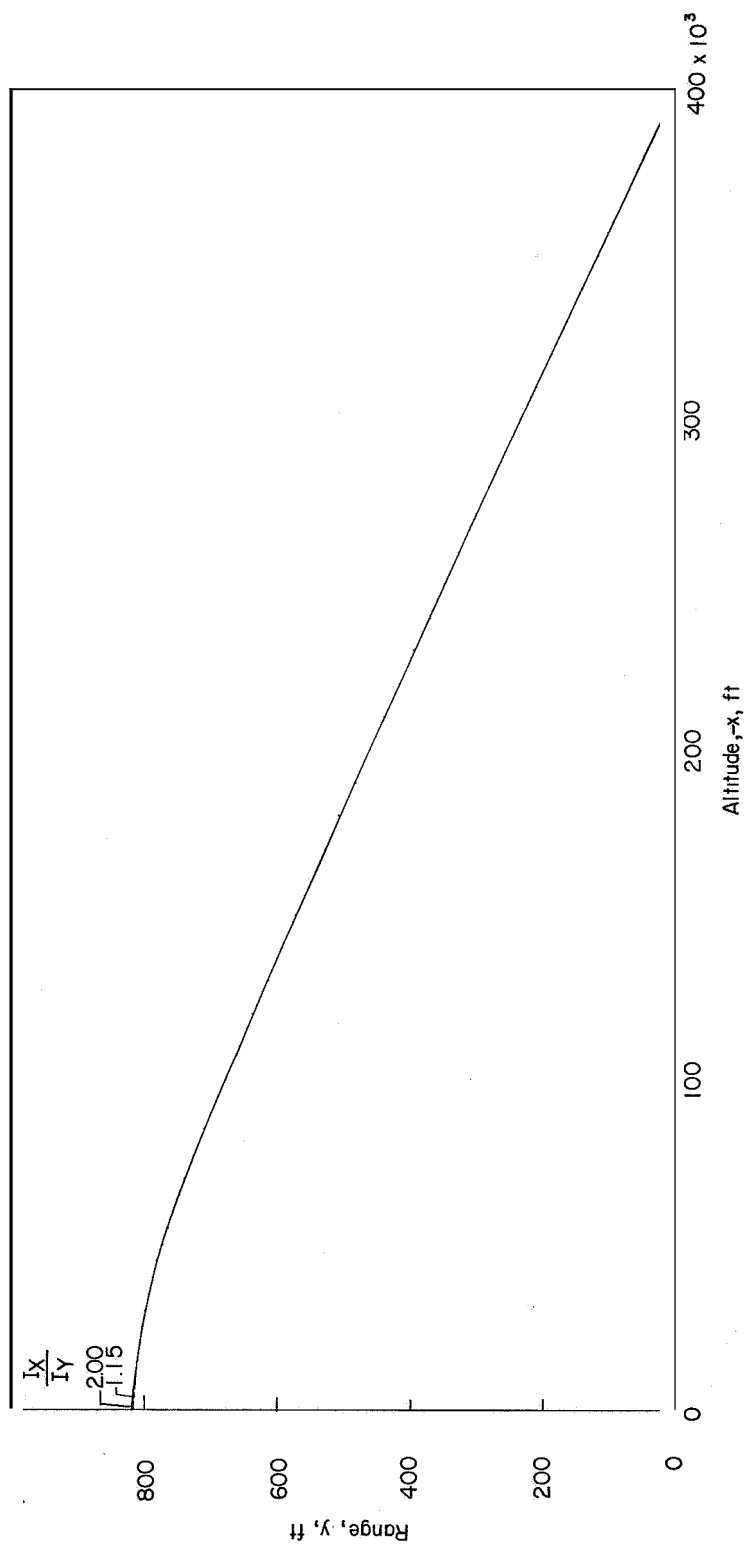**Figure** 5.- Continued.

(c) Range.

Figure 5.- Concluded.

(a) Angle of attack $\psi$ and lateral displacement.

Figure 6.- Comparison of **the** reentry behavior of shape A for two ratios of **roll** to yaw inertia. Calculations **1** and 5. $p_0 = 220$ radians/sec.

**(b)** Mach number, dynamic pressure, and time.

Figure 6.- Continued.

Altitude,-x, ft

Range, y, ft

$\dfrac{I_X}{I_Y}$

2.00
1.15

(c) Range.

Figure 6.- Concluded.